Charge-Separation Process of the $C_2H_4 + Cl_2$ Reaction in Water: ab Initio Molecular Orbital Study Using a Cluster Model

Yuzuru Kurosaki*

Advanced Photon Research Center, Japan Atomic Energy Research Institute, Umemidai, Kizu-cho, Soraku-gun, Kyoto 619-0215, Japan

Received: June 26, 2001; In Final Form: September 20, 2001

The charge-separation process of the $C_2H_4 + Cl_2$ reaction in water has been studied with ab initio molecular orbital methods using a cluster model composed of $C_2H_4 + Cl_2 + 4H_2O$. The final charge-separated complex was calculated to lie 4.3 kcal mol^{-1} lower in energy than the $C_2H_4 + Cl_2 + 4H_2O$ asymptote and 0.6 kcal mol^{-1} higher than the complex produced in the reactant region at the MP4(SDQ,full)/aug-cc-pVDZ level of theory with the zero-point energy correction and with the basis-set superposition error correction. The total free energy of the final charge-separated complex relative to the reactant complex in water at 298.15 K and 1 atm was estimated to be −5.2 kcal mol^{-1} using the gas-phase thermodynamic quantities combined with the solvation free energies obtained with the polarized continuum model. This result strongly suggests that the charge-separation process in water at the normal temperature and pressure is spontaneous.

1. Introduction

Alkene halogenation, $C_2H_4 + X_2 \rightarrow C_2H_4X_2$ (X = Cl or Br), has long been one of the most familiar reactions to organic chemists, and it is currently a well-known textbook reaction. Studies of alkene halogenation were initiated in the 1930s,[1] and it has been widely accepted that this reaction proceeds via a charge-separated species composed of a cyclic halogenium cation ($C_2H_4X^+$) and halogen anion (X^-).[2] It is expected that the charge-separation process can occur only in polar solvents but not in the gas phase. This is because in polar solvents this process can be stabilized, while in the gas phase a charge-separated asymptote usually correlates with an electronically excited potential energy surface that is not accessible under normal conditions.

It seems that even the gas-phase mechanism has not been established. Recently, we[3] have studied the gas-phase $C_2H_4 + Cl_2 \rightarrow C_2H_4Cl_2$ reaction using ab initio molecular orbital (MO) methods. Two reaction pathways were compared therein: direct Cl_2 addition to C_2H_4, which leads to the production of 1,2-dichloroethane $C_2H_4Cl_2$ (nonradical pathway); Cl abstraction from Cl_2 by C_2H_4, which leads first to the production of C_2H_4-Cl + Cl radicals and then to immediate recombination to form $C_2H_4Cl_2$ (radical pathway). The nonradical pathway was previously proposed by Yamabe et al.,[4] while the radical pathway was first examined by the present author. It was found[3] that the radical pathway is energetically more feasible than the nonradical pathway and that the radical pathway has no reaction barrier from the C_2H_4Cl + Cl side. It was calculated, however, that the reaction still needs a considerable amount of energy to proceed via the radical pathway, which makes it hard for the reaction to occur in the gas phase. We also became interested in the mechanism of the same reaction in solvents, which is expected to proceed through an energetically more feasible pathway than the gas-phase reaction.

Several theoretical studies dealing with alkene halogenation in solvents have been reported so far. Cossi et al.[5] first examined solvent effects on the charge distribution for some bromonium ions using the polarized continuum model (PCM) combined with ab initio MO theory. Rivail and co-workers[6] investigated solvent effects on the $C_2H_4 + Br_2$ reaction using discrete and continuum solvent models[6a] and using a molecular dynamics method with the quantum mechanics/molecular mechanics potentials.[6b] They[6a] thus found a marked difference between the reaction mechanisms in the gas phase and in polar solvents. Also they[6b] showed the charge-separation process into $C_2H_4Br^+ + Br^-$, in which dynamic solvent effects were found to play an important role. Recently, Amovilli et al.[7] calculated the solvation free energies for the $C_2H_4 + Cl_2 \rightarrow C_2H_4Cl^+ + Cl^-$ reaction in aqueous solution using the PCM model combined with the complete active space self-consistent-field (CASSCF) method. The exothermic energy of the reaction in aqueous solution was thus found to be quite large. Most of these studies employed continuum solvent models, which often yield reliable results for various solvated systems with a small computational cost.

It is also worthwhile to investigate alkene halogenation in solvents using the conventional way of simulating a condensed system, i.e., the cluster-model approach. In the present work, we examine the pathway for the $C_2H_4 + Cl_2 \rightarrow C_2H_4Cl^+ + Cl^-$ reaction in water using a cluster model including four H_2O molecules. Unfortunately, calculations of larger-size clusters including more than four H_2O molecules are beyond our current computational capability. We realize that the size of the model is still insufficient to adequately simulate solvent effects such as the solvation of the first-shell H_2O molecules.[6b] In addition, entropic effects on energetics, which were pointed out to be large for weakly bonded complexes in soluton,[8] cannot be accurately estimated in the present model. The cluster-model approach, however, can provide valuable insights into the microscopic mechanism for solute−solvent interaction because of the explicit consideration of solvent molecules. For example, Woon and Dunning[9] theoretically examined the water solvation

* To whom correspondence should be addressed. Tel: +81-77-471-3400. Fax: +81-77-471-3316. E-mail address: kurosaki@apr.jaeri.go.jp.

10.1021/jp012420w CCC: $20.00
Published on Web 11/10/2001

of diatomic alkali halides using similar cluster models including one to three H_2O molecules and reported some important quantities such as optimized geometries, harmonic frequencies, and energetics. We believe that the present study can be a first step for understanding the microscopic mechanism for solute−solvent interaction in alkene halogenation in water.

2. Methods of Calculation

A system consisting of C_2H_4, Cl_2, and four H_2O molecules was employed as a cluster model for the $C_2H_4 + Cl_2 \rightarrow C_2H_4Cl^+ + Cl^-$ reaction in water. Geometries of stationary points were fully optimized at the second-order Møller−Plesset perturbation (MP2)[10] level, which is based on single-reference restricted Hartree−Fock (RHF) theory under the frozen-core (fc) approximation. The employed basis set was the correlation-consistent polarized valence double-ζ (cc-pVDZ) basis set of Dunning.[11] Harmonic vibrational frequencies were computed analytically at the same level of theory and the optimized geometries were accordingly characterized as minima or saddle points of the potential energy surface. Mulliken population analyses were done at the MP2(fc)/cc-pVDZ level for the obtained stationary points. Single-point energy calculations for the optimized geometries were also performed using the fourth-order MP (MP4) method,[12] including single, double, and quadruple (SDQ) electron excitations with all electrons being included (full). For the MP4(SDQ,full) calculations, the cc-pVDZ basis set with the diffuse functions (aug-cc-pVDZ[11]) was used because the cc-pVDZ basis set overestimates the strength of hydrogen bonds because of the basis set superposition error (BSSE). The residual BSSE was estimated at the MP2(full)/aug-cc-pVDZ level using the counterpoise method.[13] The zero-point energy (ZPE) corrections at the MP2(fc)/cc-pVDZ level were included in the obtained single-point energies. The intrinsic reaction coordinate (IRC)[14] was also calculated at the MP2(fc)/cc-pVDZ level to confirm that the obtained minima and transition states (TSs) are located on a single reaction pathway. Thermodynamic quantities relative to the first minimum (denoted as M1, see below) at 298.15 K and 1 atm have been estimated using the vibrational frequencies at the MP2(fc)/cc-pVDZ level and the electronic energies at the MP4(SDQ,full)/aug-cc-pVDZ level with the BSSE correction. Finally, to obtain a rough estimate of the residual solvation energies, single-point PCM[15] calculations with the dielectric constant of 78.39 D were performed for the optimized clusters at the MP2(full)/aug-cc-pVDZ level.

For the obtained charge-separated complex, the CASSCF calculation, in which 18 electrons are distributed in 14 active orbitals (CASSCF(18,14)), was done with the cc-pVDZ basis set, thereby multi-configuration character being estimated. In this calculation, the 14 active orbitals are composed of seven a (symmetric) and seven b (antisymmetric) orbitals.

In this work, the Gaussian 94[16a] and Gaussian 98[16b] programs were used for ab initio MO methods except for the CASSCF calculation, which was carried out using the MOLCAS[17] program.

3. Results and Discussion

A. T-Shaped $C_2H_4\cdots Cl_2$ Complex. The T-shaped $C_2H_4\cdots Cl_2$ complex in the gas phase has been amply studied both theoretically[3a,18] and experimentally,[19] while only one theoretical report[7] of this complex in aqueous solution has appeared so far. The optimized geometry of the cluster model that simulates the T-shaped $C_2H_4\cdots Cl_2$ complex in water is shown in Figure 1. This is a hydrogen-bonded complex with C_2 symmetry and has been confirmed to be a minimum (M1) of the potential energy surface by harmonic vibrational analysis. All results of vibrational analyses for the optimized geometries are summarized in Table 1. It is natural to regard M1 as the starting complex for the present charge-separation process in water. For comparison, the optimized geometry calculated at the same level of theory (MP2(fc)/cc-pVDZ) for the gas-phase $C_2H_4\cdots Cl_2$ complex is displayed in Figure 1, in which the geometrical parameters for the isolated molecules, C_2H_4 and Cl_2, are also given in italic type. It is seen that in M1 the Cl−Cl distance is 0.024 Å longer, Cl−X (X is the midpoint of the C−C bond in C_2H_4) is 0.209 Å shorter, and C−C is 0.007 Å longer, as compared with the geometry of the gas-phase $C_2H_4\cdots Cl_2$ complex. In parentheses in Figure 1 are given atomic net charges obtained by Mulliken population analyses. It is predicted that in M1 both Cl atoms are negatively charged, the H atoms are positively charged, and the C atoms are negatively charged. As compared with the gas-phase $C_2H_4\cdots Cl_2$ complex, the amount of net charge for the Cl and C atoms in M1 is seen to be slightly larger; this is supplied by the H_2O molecules.

It has been predicted in the present work that the C_2H_4 molecule in water can form a hydrogen-bonded complex. The optimized geometry of the $C_2H_4\cdots 4H_2O$ complex with C_2 symmetry, which has been confirmed to be a minimum by harmonic vibrational analysis, is shown in Figure 1. In the present work, we did not consider a hydrogen-bonded complex of Cl_2 and water as a reactant complex, because the size of the cluster incorporating this complex plus the C_2H_4−water complex becomes very large, which is computationally intractable in our current computational capability. Accordingly, we assumed that in the charge-separation process simulated by the present model the formation of M1 is preceded by the formation of the $C_2H_4\cdots 4H_2O$ complex plus Cl_2 or the $C_2H_4\cdots Cl_2$ complex plus four H_2O molecules. It is noteworthy, however, that optimized geometries for hydrogen-bonded complexes of Cl_2 and water have been recently reported.[20] It is hence desirable in the future to extend the size of the present cluster model to better simulate the reaction.

Total energy values for species included in the system are given in Table 2 and the BSSEs at the MP2(full)/aug-cc-pVDZ level for the complexes are tabulated in Table 3. The ZPE-corrected relative energy values for stationary points with respect to the $C_2H_4 + Cl_2 + 4H_2O$ asymptote are summarized in Table 4. The relative energies for $C_2H_4\cdots Cl_2 + 4H_2O$, $C_2H_4\cdots 4H_2O + Cl_2$, and M1 have been calculated to be −1.1, −2.5, and −4.9 kcal mol^{-1}, respectively, at the MP4(SDQ,full)/aug-cc-pVDZ level of theory with the ZPE and BSSE corrections. One expects that the $C_2H_4\cdots Cl_2 + 4H_2O \rightarrow$ M1 process has no barrier, whereas the $C_2H_4\cdots 4H_2O + Cl_2 \rightarrow$ M1 process may have a TS, because this process includes change in the form of the hydrogen bond. Despite our effort to find the TS, the geometry optimization has been unsuccessful. We therefore assumed that the $C_2H_4\cdots 4H_2O + Cl_2 \rightarrow$ M1 process has no barrier. Because this process is characterized by change in the form of the hydrogen bond, the barrier height, if not zero, is considered to be very small. Besides, M1 has been calculated to be 6.0 kcal mol^{-1} lower in energy than $C_2H_4\cdots 4H_2O + Cl_2$ at the MP4(SDQ,full)/aug-cc-pVDZ level of theory without the BSSE correction. This means that the $C_2H_4\cdots 4H_2O + Cl_2 \rightarrow$ M1 process is classified as an "early" reaction and the barrier height is not so large. Therefore, the assumption that this process has no barrier is acceptable and does not affect the energetics for the present reaction system. It is interesting to note that the energy of the $C_2H_4\cdots 4H_2O$ complex is seen to be greatly

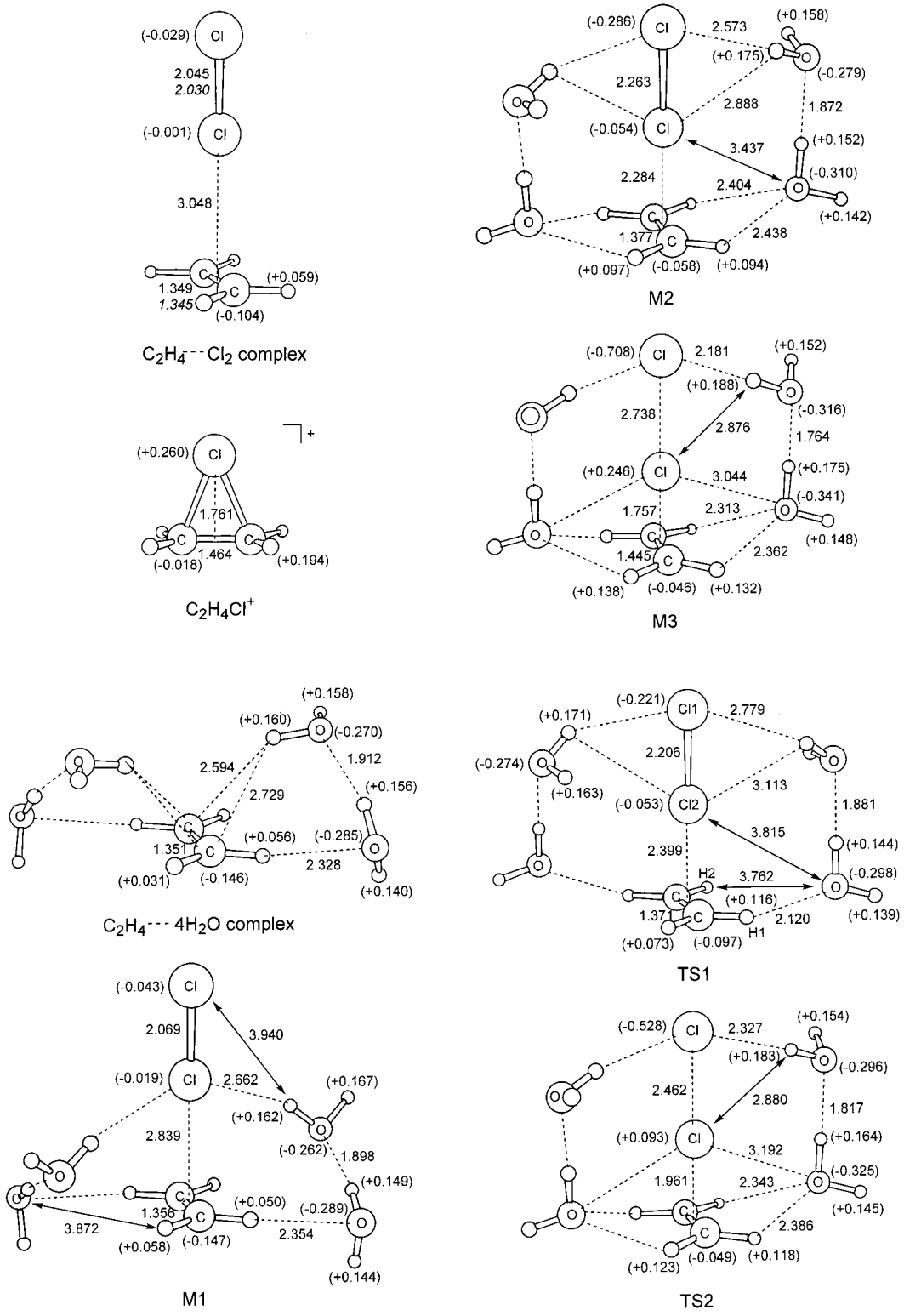

Figure 1. Optimized geometries calculated at the MP2(fc)/cc-pVDZ level of theory. In parentheses are given atomic net charges. The optimized values for the bond lengths of the isolated C_2H_4 and Cl_2 molecules are given in italic type. Bond lengths are given in Å.

affected by the inclusion of diffuse functions in the basis set, while it is not so affected by raising the theoretical level of the electron-correlation method; the MP2(fc)/cc-pVDZ method has predicted the $C_2H_4\cdots 4H_2O + Cl_2$ relative energy to be more than 2 times larger than that predicted by the MP2(full)/aug-cc-pVDZ method, while the MP4(SDQ,full)/aug-cc-pVDZ method has yielded a value close to that from the MP2(full)/aug-cc-pVDZ method. This suggests that the BSSE is large for the $C_2H_4\cdots 4H_2O$ complex when the basis set without diffuse functions is used. On the other hand, the electron-correlation effect on the energy of M1 is seen to be relatively large. It has been found, however, that despite the use of the basis set including diffuse functions the residual BSSEs for both $C_2H_4\cdot\cdot\cdot 4H_2O$ and M1 are not so small.

B. Another $C_2H_4\cdots Cl_2$ Complex. Another hydrogen-bonded $C_2H_4\cdots Cl_2$ complex with C_2 symmetry has been optimized and harmonic vibrational analysis has verified that it is located at a minimum (M2). It is seen in the geometry of M2 shown in

TABLE 1: Harmonic Vibrational Frequencies and ZPEs for the Optimized Geometries Calculated at the MP2(fc)/cc-pVDZ Level of Theory

	sym	frequencies (cm^{-1})														ZPE (hartree)
Cl_2	$D_{\infty h}$	548 (σ_g)														0.001 25
H_2O	C_{2v}	1678 (a_1)	3853 (a_1)	3972 (b_2)												0.021 65
C_2H_4	C_{2h}	826 (b_{2u})	936 (b_{2g})	973 (b_{3u})	1066 (a_u)	1236 (b_{3g})	1376 (a_g)	1467 (b_{1u})	1688 (a_g)	3187 (b_{1u})	3206 (a_g)	3285 (b_{3g})	3311 (b_{2u})			0.051 39
$C_2H_4\cdots Cl_2$	C_{2v}	63 (b_1) 3188 (b_2)	64(b_2) 3205 (a_1)	84 (a_1) 3287 (a_2)	97 (b_2) 3313 (b_1)	137 (b_1)	517 (a_1)	826 (b_1)	939 (b_2)	980 (a_1)	1060 (a_2)	1236 (a_2)	1373 (a_1)	1467 (b_2)	1677 (a_1)	0.053 56
$C_2H_4\cdots 4H_2O$	C_2	24 (a) 217 (a) 1249 (a) 3832 (b)	30 (b) 219 (b) 1389 (a) 3834 (a)	35 (a) 253 (a) 1484 (b) 3919 (b)	69 (a) 302 (b) 1666 (a) 3919 (a)	69 (b) 350 (b) 1669 (b) 3947 (b)	106 (a) 350 (a) 1675 (a) 3950 (a)	107 (b) 389 (a) 1709 (b)	155 (b) 393 (b) 1709 (a)	158 (b) 696 (b) 3171 (b)	161 (a) 706 (a) 3183 (a)	184 (b) 861 (b) 3278 (a)	189 (a) 1016 (b) 3298 (b)	203 (a) 1031 (a) 3752 (b)	204 (b) 1149 (a) 3752 (a)	0.150 38
M1	C_2	23 (b) 175 (a) 721 (b) 3177 (b)	32 (a) 186 (a) 730 (a) 3189 (a)	33 (b) 201 (b) 877 (b) 3286 (a)	44 (b) 210 (a) 1029 (b) 3307 (b)	47 (a) 212 (b) 1051 (a) 3746 (b)	71 (a) 224 (a) 1139 (a) 3746 (a)	86 (b) 243 (b) 1265 (a) 3825 (b)	91 (a) 259 (a) 1384 (a) 3826 (a)	100 (b) 284 (b) 1488 (b) 3917 (b)	108 (a) 294 (a) 1659 (a) 3917 (a)	125 (b) 409 (b) 1667 (b) 3939 (b)	132 (b) 415 (a) 1669 (a) 3941 (a)	163 (b) 426 (b) 1715 (b)	172 (b) 465 (a) 1716 (a)	0.153 00
M2	C_2	22 (b) 181 (b) 765 (a) 3198 (b)	28 (a) 196 (b) 767 (b) 3203 (a)	56 (a) 204 (a) 846 (b) 3323 (a)	57 (b) 215 (a) 1036 (a) 3342 (b)	62 (b) 222 (b) 1042 (b) 3677 (b)	89 (a) 242 (a) 1067 (a) 3678 (a)	98 (b) 242 (b) 1254 (a) 3817 (b)	119 (a) 257 (b) 1340 (a) 3818 (a)	129 (b) 320 (a) 1415 (b) 3921 (b)	133 (a) 356 (b) 1589 (a) 3921 (a)	142 (b) 363 (a) 1684 (b) 3921 (b)	144 (a) 493 (b) 1687 (a) 3922 (a)	163 (b) 516 (a) 1712 (b)	181 (a) 582 (b) 1713 (a)	0.153 70
M3	C_2	12 (b) 221 (b) 868 (a) 3201 (a)	41 (a) 238 (b) 868 (b) 3201 (b)	49 (b) 244 (a) 968 (b) 3337 (a)	82 (b) 265 (a) 1012 (a) 3350 (b)	91 (a) 281 (b) 1145 (a) 3478 (b)	91 (b) 378 (b) 1161 (b) 3496 (a)	118 (a) 385 (a) 1240 (a) 3572 (b)	159 (a) 454 (a) 1247 (a) 3588 (a)	174 (a) 497 (b) 1395 (b) 3898 (b)	175 (b) 511 (a) 1484 (a) 3899 (a)	181 (b) 557 (b) 1704 (b) 3917 (b)	198 (a) 729 (a) 1709 (a) 3917 (a)	201 (b) 729 (b) 1736 (b)	203 (a) 858 (b) 1739 (a)	0.157 77
TS1	C_2	62i (a) 151 (b) 732 (b) 3165 (b)	56i (b) 171 (a) 732 (a) 3174 (a)	6 (b) 185 (b) 865 (b) 3284 (a)	22 (a) 188 (b) 1027 (a) 3303 (b)	23 (b) 191 (a) 1037 (b) 3703 (b)	30 (a) 220 (b) 1109 (a) 3704 (a)	61 (b) 225 (a) 1251 (a) 3836 (b)	61 (a) 231 (b) 1367 (a) 3836 (a)	93 (a) 326 (a) 1474 (b) 3930 (b)	112 (b) 327 (b) 1623 (a) 3930 (a)	122 (b) 336 (a) 1679 (b) 3932 (a)	127 (a) 454 (b) 1686 (a) 3932 (b)	138 (b) 486 (a) 1711 (b)	149 (a) 513 (b) 1712 (a)	0.151 90
TS2	C_2	200i (a) 206 (b) 821 (a) 3202 (b)	24 (b) 219 (b) 823 (b) 3203 (a)	38 (a) 227 (a) 852 (b) 3334 (a)	66 (b) 240 (a) 1011 (a) 3350 (b)	81 (a) 260 (b) 1096 (a) 3591 (b)	85 (b) 286 (a) 1101 (b) 3595 (a)	122 (b) 307 (b) 1250 (a) 3720 (b)	138 (a) 311 (a) 1295 (a) 3728 (a)	150 (a) 409 (b) 1404 (b) 3903 (b)	153 (b) 438 (b) 1532 (a) 3904 (a)	156 (a) 445 (a) 1695 (b) 3918 (b)	171 (b) 623 (b) 1698 (a) 3918 (a)	182 (a) 632 (a) 1724 (b)	188 (b) 802 (b) 1726 (a)	0.155 72

TABLE 2: Total Energies (hartree) for the MP2(fc)/cc-pVDZ Geometries

	MP2(fc)/cc-pVDZ	MP2(full)/aug-cc-pVDZ	MP4(SDQ,full)/aug-cc-pVDZ
Cl_2	−919.231 96	−919.273 69	−919.297 77
H_2O	−76.228 67	−76.263 28	−76.270 94
C_2H_4	−78.315 30	−78.334 39	−78.362 51
$C_2H_4\cdots Cl_2$	−997.551 43	−997.615 33	−997.665 29
$C_2H_4\cdots 4H_2O$	−383.273 78	−383.414 45	−383.470 85
M1	−1302.514 46	−1302.703 29	−1302.779 52
M2	−1302.514 01	−1302.713 66	−1302.778 95
M3	−1302.513 94	−1302.718 63	−1302.786 50
TS1	−1302.510 83	−1302.708 36	−1302.776 65
TS2	−1302.512 02	−1302.715 88	−1302.782 21

TABLE 3: BSSE (hartree) at the MP2(full)/aug-cc-pVDZ Level

	fragment[a]	uncounter-poise	counter-poise	ΔE	total
$C_2H_4\cdots Cl_2$	C_2H_4	−78.334 39	−78.335 33	0.000 94	0.002 40
	Cl_2	−919.273 70	−919.275 16	0.001 46	
$C_2H_4\cdots 4H_2O$	C_2H_4	−78.334 21	−78.336 33	0.002 12	0.008 16
	H_2O(A)	−76.263 23	−76.264 60	0.001 37	
	H_2O(B)	−76.263 36	−76.265 01	0.001 65	
M1	C_2H_4	−78.334 22	−78.336 94	0.002 72	0.013 87
	Cl_2	−919.273 42	−919.278 09	0.004 67	
	H_2O(A)	−76.263 23	−76.264 60	0.001 37	
	H_2O(B)	−76.263 36	−76.265 01	0.001 65	
M2	C_2H_4	−78.332 74	−78.335 80	0.003 06	0.018 26
	Cl_2	−919.261 61	−919.270 25	0.008 64	
	H_2O(A)	−76.263 20	−76.264 79	0.001 59	
	H_2O(B)	−76.263 19	−76.264 88	0.001 69	
M3	$C_2H_4Cl^+$	−537.679 69	−537.683 93	0.004 24	0.017 01
	Cl^-	−459.729 38	−459.734 21	0.004 83	
	H_2O(A)	−76.262 96	−76.264 83	0.001 87	
	H_2O(B)	−76.262 87	−76.264 97	0.002 10	
TS1	C_2H_4	−78.333 59	−78.336 41	0.002 82	0.015 98
	Cl_2	−919.266 37	−919.273 39	0.007 02	
	H_2O(A)	−76.263 24	−76.264 73	0.001 49	
	H_2O(B)	−76.263 16	−76.264 74	0.001 58	
TS2	$C_2H_4Cl^+$	−537.665 91	−537.670 30	0.004 39	0.016 73
	Cl^-	−459.729 38	−459.734 38	0.005 00	
	H_2O(A)	−76.263 11	−76.264 86	0.001 75	
	H_2O(B)	−76.263 10	−76.265 02	0.001 92	

[a] H_2O(A) and H_2O(B) are each one of the two equivalent H_2O molecules.

Figure 1 that the Cl−Cl and Cl−X distances apparently change from those for M1; the Cl−Cl distance has been calculated to be 2.263 Å and the Cl−X distance 2.284 Å in M2. Atomic net charges also considerably change from those for M1; in particular, the upper Cl atom is more negatively charged, the H atoms in C_2H_4 are more positively charged, and the C atoms in C_2H_4 are less negatively charged, as compared with M1. Judging from the bond lengths and atomic net charges, however, in M2, the Cl−Cl bond is still not completely broken and the two C−Cl bonds are still not completely formed. The most striking change in geometry from M1 to M2 is the form of the hydrogen bond; in M1, H's of the upper H_2O's form hydrogen bonds with only the lower Cl, whereas in M2, H's of the upper H_2O's form hydrogen bonds with both the upper and lower Cl's. In M1, O's of the lower H_2O's are seen to form hydrogen bonds with one H of C_2H_4, whereas in M2, the same O's form hydrogen bonds with two H's.

The optimized geometry of the TS (TS1), which has C_2 symmetry of point group, for conversion from M1 to M2 is displayed in Figure 1. As shown in Table 1, harmonic vibrational analysis has revealed that TS1 has two imaginary frequency modes with a (symmetric) and b (anti-symmetric) symmetries, i.e., TS1 is located at a second-order saddle point. This means that there is a real TS with C_1 symmetry, which is lower in energy than TS1. However, we did not reoptimize the C_1 TS, because the reoptimization at the same level of theory requires an extremely high cost of computation and because, as mentioned just below, the energy difference between M1 and TS1 has already been predicted to be quite small, meaning that obtaining the C_1 TS geometry and energy does not significantly affect the energetics. It is seen in TS1 that the upper four hydrogen bonds between Cl's and H's are being formed, while the lower hydrogen bonds between O's and H's are still similar in form to those in M1. It is interesting to note that the lengths of the lower hydrogen bonds between O's and H's in TS1 were slightly shorter than those in M1 and M2.

Relative energies for the conversion from M1 to M2 via TS1 are given in Table 4. It has been estimated that TS1 is 2.4 kcal mol^{-1} higher in energy than M1 but 1.1 kcal mol^{-1} lower than M2 at the MP4(SDQ,full)/aug-cc-pVDZ level with the ZPE and BSSE corrections. The electron-correlation effects are seen to be larger than the basis-set effects for both TS1 and M2; the difference between the MP2(fc)/cc-pVDZ and MP2(full)/aug-cc-pVDZ results is small, while that between MP2(full)/aug-cc-pVDZ and MP4(SDQ,full)/aug-cc-pVDZ is large. However, the residual BSSEs are seen to be quite large for both TS1 and M2.

In Figure 2 are shown the potential energy profile and geometrical parameters along the IRC for the conversion from M1 to M2 via TS1. The absolute value of s gives the arc length of the IRC measured from TS1 that is situated at $s = 0$, and M1 and M2 are in the $s < 0$ and $s > 0$ regions, respectively. The potential energy is given in kcal mol^{-1} relative to the total energy of M2. The numbering for atoms in Figure 2b are given in the geometry of TS1 in Figure 1. We had to stop calculating the IRC from TS1 to M1 halfway around $s = -4$ $amu^{1/2}$ bohr as shown in Figure 2. This is because the entire IRC from TS1 to M1 is quite a long way and the gradient of the IRC is too small to accurately calculate. The variation in bond lengths along the IRC in the $s < 0$ region, however, implies that the IRC would finally reach M1 if the calculation were completed. On the other hand, the IRC from TS1 to M2 has been completely calculated, as clearly shown in Figure 2, although this is also computationally demanding. It has been confirmed that the potential energy in the $s > 0$ region finally reaches the total energy of M2 and the bond lengths reach those of M2 (see Figure 1). It is interesting to note that the H−Cl2 distance reaches 3.6 Å around $s = -4$ $amu^{1/2}$ bohr, while it has been calculated to be 2.662 Å in M1. This means that the H−Cl2

TABLE 4: Relative Energies (kcal mol^{-1}) with the ZPE Correction at the MP2(fc)/cc-pVDZ Level

	$C_2H_4 + Cl_2 + 4H_2O$	$C_2H_4\cdots Cl_2 + 4H_2O$	$C_2H_4\cdots 4H_2O + Cl_2$	M1	TS1	M2	TS2	M3
MP2(fc)/cc-pVDZ	0.0	−2.0	−19.7	−24.3	−22.7	−23.6	−21.1	−21.0
MP2(full)/aug-cc-pVDZ	0.0	−3.9	−9.1	−17.8	−21.6	−23.8	−24.0	−24.4
MP4(SDQ,full)/aug-cc-pVDZ	0.0	−2.6	−7.6	−13.6	−12.5	−12.8	−13.6	−15.0
MP4(SDQ,full)/aug-cc-pVDZ[a]	0.0	−1.1	−2.5	−4.9	−2.5	−1.4	−3.1	−4.3

[a] The BSSE correction at the MP2(full)/aug-cc-pVDZ level is included.

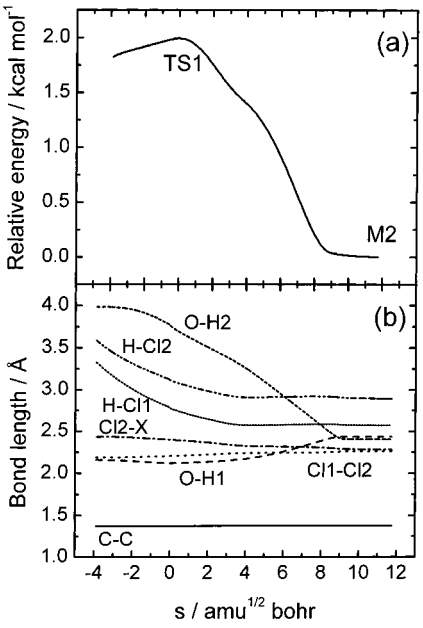

Figure 2. Variation in properties along the IRC for the M1 → M2 conversion: (a) potential energy; (b) geometrical parameters. The abscissa is common for parts a and b and represents *s* the absolute value of which corresponds to the arc length of the IRC measured from TS1. M1 and M2 are situated in the $s < 0$ and $0 < s$ regions, respectively, and TS1 is at $s = 0$. X is the midpoint of the C−C bond.

distance has a maximum value on the reaction pathway between $s = -4$ amu$^{1/2}$ bohr and M1. It is also noteworthy that the O−H1 distance has a minimum value around TS1, as suggested above. Although the IRC calculation is incomplete in the M1 region, one can thus safely conclude that M1, TS1, and M2 are connected with each other through a single reaction pathway.

C. Charge-Separated Complex. The optimized geometry of the charge-separated complex is pictured in Figure 1, which has been predicted to be a minimum (M3) by harmonic vibrational analysis. M3 is regarded as the final complex of the charge-separation process examined in the present study. Although the form of the hydrogen bond in M3 seems similar to that in M2, it is seen that in M3 the Cl−Cl bond completely breaks and the two C−Cl bonds completely form; the Cl−Cl and Cl−X distances have been calculated to be 2.738 and 1.757 Å, respectively. It is interesting to note that Amovilli et al.,[7] predicted the Cl−Cl distance in the charge-separated complex to be 3.235 Å using the PCM model combined with the CASSCF method, which is considerably larger than the one in the present calculation. This may be mainly due to the difference in the employed model; we directly optimized the $C_2H_4Cl_2 + 4H_2O$ cluster, while Amovilli et al. employed the PCM model for the $C_2H_4Cl_2$ system and, presumably, the charge-separated complex was predicted to more strongly interact with water. The net charges for the upper and lower Cl atoms have been predicted to be −0.708 and +0.246. This result suggests that the upper Cl is almost the Cl^- anion. The distances between the lower Cl and the O's of the lower H_2O's have been calculated to be 3.044 Å, and hence, the electrostatic attractive force between Cl and O's is considered to be relatively strong. It is clear that the geometry and charge distribution of a small cluster in M3, constructed from the lower Cl and C_2H_4, are quite similar to those of the gas-phase cyclic $C_2H_4Cl^+$ cation of which the optimized geometry and atomic net charges are also depicted in Figure 1. One may thus conclusively state that M3 simulates a hydrogen-bonded charge-separated $C_2H_4Cl^+\cdots Cl^-$ complex in water.

TABLE 5: Relative Thermodynamic Quantities (kcal mol^{-1}) at 298.15 K and 1 atm[a]

	M1	TS1	M2	TS2	M3
$\Delta(H-E)$	0.0	−1.4	0.0	0.1	1.0
$-T\Delta S$	0.0	0.5	2.0	5.6	5.6
ΔG^b	0.0	2.2	5.1	5.7	4.1

[a] Enthalpic and entropic contributions are calculated using vibrational frequencies at the MP2(fc)/cc-pVDZ level. [b] Relative free energies are obtained using electronic energies at the MP4(SDQ,full)/aug-cc-pVDZ level with the BSSE correction at the MP2(full)/aug-cc-pVDZ level.

The optimized geometry of the TS (TS2), which has C_2 symmetry of point group, for conversion from M2 to M3 is shown also in Figure 1. Harmonic vibrational analysis predicts, as shown in Table 1, that TS2 has one imaginary frequency mode. The geometrical parameters and atomic net charges for TS2 are seen to be midway between M2 and M3. It is interesting to note that the net charge of the lower Cl has been calculated to be slightly positive at this point; therefore, a weak attractive force due to electrostatic interaction already works between the lower Cl and the O's of the lower H_2O's.

Relative energy values for the conversion from M2 to M3 via TS2 are also given in Table 4. TS2 has been evaluated to lie 1.2 kcal mol^{-1} higher in energy than M3, but 1.7 kcal mol^{-1} lower than M2, at the MP4(SDQ,full)/aug-cc-pVDZ level with the ZPE and BSSE corrections. Again, the electron-correlation effects and residual BSSEs have been estimated to be large for both TS2 and M3. It has been theoretically shown that TS2 and M3 are 3.1 and 4.3 kcal mol^{-1} lower than the $C_2H_4 + Cl_2 + 4H_2O$ asymptote at the MP4(SDQ,full)/aug-cc-pVDZ level with the ZPE and BSSE corrections. Because the energies of complexes TS1−M3 are seen to be comparable with the energy of M1, it is thought that the M1 → M3 charge-separation process can easily occur at low temperatures. At around room temperature, however, entropic effects on energetics are not considered to be negligible and this conclusion does not always hold. Thermodynamic quantities relative to M1 at 298.15 K and 1 atm are summarized in Table 5. It is clear that entropic terms, $-T\Delta S$, for TS2 and M3 are relatively large, which leads to the positive value for the relative free energy ΔG for M3. This means that the M1 → M3 charge-separation process is disfavored at room temperature. It is not expected, however, that the present cluster model has accurately calculated entropy variations in water; accurate calculations of entropic effects in solution would require that a much larger-size cluster is employed and the $C_2H_4 + Cl_2$ system is completely involved in the hydrogen-bond network of the cluster throughout the entire reaction from the reactant to product. It is possible that such a cluster model would yield a smaller value of $-T\Delta S$ for M3, which makes the charge-separation process spontaneous even around room temperature.

In Figure 3 is shown the result of the IRC calculation for the M2 → M3 conversion via TS2: part a shows the potential energy profile; part b shows the geometrical parameters. TS2 is situated at $s = 0$ and M2 and M3 are in the $s < 0$ and $s > 0$ regions, respectively. The potential energy is given in kcal mol^{-1} relative to the total energy of M2. It has been verified that the potential energy curve along the IRC smoothly connects the total energy of M2 with that of M3. The Cl−Cl and Cl−X distances are seen to smoothly change from those of M2 to those of M3 along the IRC. It is therefore concluded that M2, TS2, and M3 are on a single reaction pathway.

One may suspect that the ionic electronic structure of M3 was incorrectly predicted, because it is well-known that the RHF method for a prolonged single bond incorrectly gives ionic

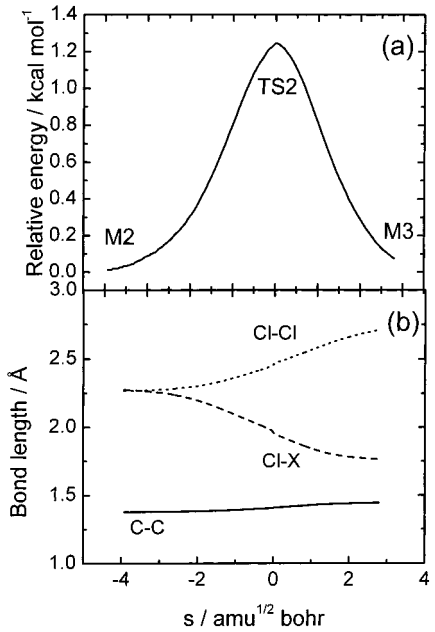

Figure 3. Variation in properties along the IRC for the M2 → M3 conversion: (a) potential energy; (b) geometrical parameters. M2 and M3 are situated in the $s < 0$ and $0 < s$ regions, respectively, and TS2 is at $s = 0$. X is the midpoint of the C−C bond.

separation. When the RHF method gives a wrong result, an unrestricted HF (UHF) wave function is expected to predict a lower energy value, because the UHF method can present a qualitatively correct description for nonionic (i.e., radical) separation of a single bond. The situation that the UHF wave function gives lower energy than RHF is called RHF−UHF instability, which, in general, originates from the multiconfiguration character of the electronic structure. Therefore multiconfiguration SCF (MCSCF) calculations should be performed to decide between ionic and nonionic separations. In the present study, first, we have tried to obtain a UHF wave function for M3 that gives a lower energy value than RHF; however, such a UHF solution could not be found. Next, we have done a MCSCF calculation for M3 at the CASSCF(18,14)/cc-pVDZ level of theory. Consequently, the weight (i.e., the square of the coefficient) of the single-reference HF configuration in the CASSCF wave function was found to be 0.941, which is close to unity. This result strongly suggests that single-reference-based theory well describes the electronic structures of M3. Therefore one may conclude that the electronic structure of M3 is ionic and that the present single-reference-based methods, MP2 and MP4(SDQ), can be safely used not only for M3 but also for the other stationary points situated on the reaction pathway leading to M3.

D. PCM Calculation. Because it is not possible to enlarge the size of the present cluster model, we have carried out single-point PCM calculations for the obtained complexes M1−M3, thereby roughly estimating the residual solvent effects that were overlooked in the present cluster calculation. Total energies, solvation free energies (ΔG_{solv}), and total relative free energies (ΔG_{tot}) for the complexes are given in Table 6. ΔG_{solv} is defined as the difference in the energy of the complex in water and in the gas phase. Note that ΔG_{tot} has been evaluated from ΔG_{solv} combined with the gas-phase thermodynamic quantities given in Table 5. ΔG_{solv}'s for M1, TS1, M2, TS2, and M3 have been calculated to be −4.0, −2.5, −2.4, −7.6, and −13.0 kcal mol^{-1}, respectively. It should be noted that ΔG_{solv} for M3 has been predicted to be the largest: 13.0 kcal mol^{-1}. This is due to the fact that charge-separated species are greatly stabilized by a polar medium. The present result for ΔG_{solv} is in qualitative accord with the theoretical prediction of Amovilli et al.,[7] using the PCM model combined with the CASSCF method, that the solvation free energy for $C_2H_4Cl^+ + Cl^-$ is 46.2 kcal mol^{-1} in water at 298 K, although the estimated value is considerably larger than the present result for M3. ΔG_{tot}'s with respect to M1 for TS1, M2, TS2, and M3 have been evaluated to be 3.3, 6.3, 1.7, and −5.2 kcal mol^{-1}, respectively. It is noteworthy that calculated ΔG_{tot} for M3 is negative, meaning that the charge-separation process is spontaneous at room temperature. In the present PCM calculation, geometies in solution were not optimized; therefore, obtained ΔG_{solv}'s are smaller than the true values at the employed level of theory. It is preferable that vibrational analyses are performed for the optimized geometries in solution and the results are used for the free energy evaluation; unfortunately, this is beyond our current computational capability. It is quite encouraging, however, that ΔG_{tot} for M3 was estimated to be negative in the present study.

4. Conclusions

In the present study, the charge-separation process of the $C_2H_4 + Cl_2$ reaction in water has been studied using ab initio MO methods. A cluster model composed of $C_2H_4 + Cl_2 + 4H_2O$ was employed to simulate the reaction. Two TSs (TS1 and TS2) and three minima (M1−M3) were optimized, and they were confirmed to be on a single reaction pathway by IRC analysis. TS1 was found to be the TS for change in the form of the hydrogen bond from the T-shaped $C_2H_4\cdots Cl_2$ complex M1 to another T-shaped complex, M2. TS2 was found to be the TS for the formation of the charge-separated complex M3 from M2. The energy of M3 was calculated to be −4.3 kcal mol^{-1} relative to the $C_2H_4 + Cl_2 + 4H_2O$ asymptote and 0.6 kcal mol^{-1} relative to M1 at the MP4(SDQ,full)/aug-cc-pVDZ level of theory with the ZPE and BSSE corrections. Because the energies for M1−M3 were found to be comparable, the charge-separation M1 → M3 process can occur at low temperatures where entropic effects are negligible.

To estimate the energetics at the room temperature, thermodynamic quantities at 298.15 K and 1 atm were calculated using the vibrational frequencies at the MP2(fc)/cc-pVDZ level and electronic energies at the MP4(SDQ,full)/aug-cc-pVDZ level with the BSSE correction. The free energy for M3 relative to M1 was evaluated to be 4.2 kcal mol^{-1}, suggesting that this *gas-phase* process is unfavorable. Moreover, single-point PCM calculations for M1−M3 were carried out at the MP2(full)/aug-cc-pVDZ level and solvation free energies were estimated. Total

TABLE 6: Total Energies (hartree), Solvation Free Energies (ΔG_{solv}, kcal mol^{-1}), and Total Relative Free Energies (ΔG_{tot}, kcal mol^{-1}) for Complexes M1−M3 in Water Calculated Using the PCM Model at the MP2(full)/aug-cc-pVDZ Level

	M1	TS1	M2	TS2	M3
total	−1302.709 70	−1302.712 41	−1302.717 49	−1302.728 03	−1302.739 38
ΔG_{solv}[a]	−4.0	−2.5	−2.4	−7.6	−13.0
ΔG_{tot}[b]	0.0	3.3	6.3	1.7	−5.2

[a] Difference in energy between complexes in water and in the gas phase. Energies in the gas phase at the same level of theory are given in Table 2. [b] Evaluated from ΔG_{solv} combined with the gas-phase values given in Table 5.

relative free energies were thus evaluated using the solvation free energies combined with the gas-phase free energies. As a result, the total free energy for M3 relative to M1 was estimated to be -5.2 kcal mol^{-1}. This implies that the present charge-separation process in water is spontaneous.

The CASSCF(18,14)/cc-pVDZ calculation was carried out for M3 to estimate the amount of multiconfiguration character. Consequently, the weight of the single-reference HF wave function was found to be close to unity, indicating that the HF-based methods, MP2 and MP4(SDQ), describe the electronic structure of M3 qualitatively well. Moreover, this result suggests that the MP2 and MP4(SDQ) methods are suitable for calculating the entire reaction pathway of the present reaction system.

One may think that the present cluster model is still incapable of well describing the charge-separation process of the title reaction in polar solvents. We believe, however, that the present theoretical result can be a first step for understanding the microscopic mechanism for solute−solvent interaction in alkene halogenation in water.

Supporting Information Available: Cartesian coordinates (Å) for the MP2(fc)/cc-pVDZ geometries for the stationary points and fragments. This material is available free of charge via the Internet at http://pubs.acs.org.

References and Notes

(1) (a)Bartlett, P. D.; Tarbell, D. S. *J. Am. Chem. Soc.* **1936**, *58*, 466. (b) Roberts, I.; Kimball, G. E. *J. Am. Chem. Soc.* **1937**, *59*, 947.

(2) (a) Dubois, J. E.; Garnier, F. *Spectrochim. Acta, Part A* **1967**, *23*, 2279. (b) Olah, G. A.; Bollinger, J. M. *J. Am. Chem. Soc.* **1968**, *90*, 947. (c) Ruasse, M. F.; Dubois, J. E. *J. Am. Chem. Soc.* **1975**, *97* 1977. (d) Brown, R. S.; Slebocka-Tilk, H.; Bennet, A. J.; Bellucci, G.; Bianchini, R.; Ambrosetti, R. *J. Am. Chem. Soc.* **1990**, *112*, 6310. (e) Ruasse, M. F. *Acc. Chem. Res.* **1990**, *23*, 87.

(3) (a) Kurosaki, Y. *J. Mol. Struct.: THEOCHEM* **2000**, *503*, 231. (b) Kurosaki, Y. *J. Mol. Struct.: THEOCHEM* **2001**, *545*, 225.

(4) Yamabe, S.; Minato, T.; Inagaki, S. *J. Chem. Soc., Chem. Commun.* **1988**, 532.

(5) Cossi, M.; Persico, M.; Tomasi, J. *J. Am. Chem. Soc.* **1994**, *116*, 5373.

(6) (a) Assfeld, X.; Garapon, J.; Rinaldi, D.; Ruiz-Lopez, M.-F.; Rivail, J. L. *J. Mol. Struct.: THEOCHEM* **1996**, *371*, 107. (b) Strnad, M.; Martins-Costa, M. T. C.; Millot, C.; Tuñón, I.; Ruiz-López, M. F.; Rivail, J. L. *J. Chem. Phys.* **1997**, *106*, 3643.

(7) Amovilli, C.; Floris, F. M.; Mennucci, B. *Int. J. Quantum Chem.* **1999**, *74*, 59.

(8) Antonczak, S.; Ruiz-Lopez, M. F.; Rivail, J. L. *J. Am. Chem. Soc.* **1994**, *116*, 3912.

(9) Woon, D. E.; Dunning, T. H., Jr. *J. Am. Chem. Soc.* **1995**, *117*, 1090.

(10) (a) Head-Gordon, M.; Pople, J. A.; Frisch, M. J. *Chem. Phys. Lett.* **1988**, *153*, 503. (b) Frisch, M. J.; Head-Gordon, M.; Pople, J. A. *Chem. Phys. Lett.* **1990**, *166*, 275. (c) Frisch, M. J.; Head-Gordon, M.; Pople, J. A. *Chem. Phys. Lett.* **1990**, *166*, 281.

(11) Dunning, T. H., Jr. *J. Chem. Phys.* **1989**, *90*, 1007.

(12) (a) Krishnan, R.; Pople, J. A. *Int. J. Quantum Chem.* **1978**, *14*, 91. (b) Krishnan, R.; Frisch, M. J.; Pople, J. A. *J. Chem. Phys.* **1980**, *72*, 4244.

(13) Boys, S. F.; Bernardi, F. *Mol. Phys.* **1970**, *19*, 553.

(14) (a) Fukui, K. *J. Phys. Chem.* **1970**, *74*, 4161. (b) Gonzalez, C.; Schlegel, H. B. *J. Chem. Phys.* **1989**, *90*, 2154. (c) Gonzalez, C.; Schlegel, H. B. *J. Phys. Chem.* **1990**, *94*, 5523.

(15) (a) Miertus, S.; Scrocco, E.; Tomasi, J. *Chem. Phys.* **1981**, *55*, 117. (b) Miertus, S.; Tomasi, J. *Chem. Phys.* **1982**, *65*, 239.

(16) (a) Frisch, M. J.; Trucks, G. W.; Schlegel, H. B.; Gill, P. M. W.; Johnson, B. G.; Robb, M. A.; Cheeseman, J. R.; Keith, T.; Petersson, G. A.; Montgomery, J. A.; Raghavachari, K.; Al-Laham, M. A.; Zakrzewski, V. G.; Ortiz, J. V.; Foresman, J. B.; Cioslowski, J.; Stefanov, B. B.; Nanayakkara, A.; Challacombe, M.; Peng, C. Y.; Ayala, P. Y.; Chen, W.; Wong, M. W.; Andres, J. L.; Replogle, E. S.; Gomperts, R.; Martin, R. L.; Fox, D. J.; Binkley, J. S.; Defrees, D. J.; Baker, J.; Stewart, J. P.; Head-Gordon, M.; Gonzalez, C.; Pople, J. A. *Gaussian 94*, revision D.3; Gaussian, Inc.: Pittsburgh, PA, 1995. (b) Frisch, M. J.; Trucks, G. W.; Schlegel, H. B.; Scuseria, G. E.; Robb, M. A.; Cheeseman, J. R.; Zakrzewski, V. G.; Montgomery, J. A., Jr.; Stratmann, R. E.; Burant, J. C.; Dapprich, S.; Millam, J. M.; Daniels, A. D.; Kudin, K. N.; Strain, M. C.; Farkas, O.; Tomasi, J.; Barone, V.; Cossi, M.; Cammi, R.; Mennucci, B.; Pomelli, C.; Adamo, C.; Clifford, S.; Ochterski, J.; Petersson, G. A.; Ayala, P. Y.; Cui, Q.; Morokuma, K.; Malick, D. K.; Rabuck, A. D.; Raghavachari, K.; Foresman, J. B.; Cioslowski, J.; Ortiz, J. V.; Stefanov, B. B.; Liu, G.; Liashenko, A.; Piskorz, P.; Komaromi, I.; Gomperts, R.; Martin, R. L.; Fox, D. J.; Keith, T.; Al-Laham, M. A.; Peng, C. Y.; Nanayakkara, A.; Gonzalez, C.; Challacombe, M.; Gill, P. M. W.; Johnson, B. G.; Chen, W.; Wong, M. W.; Andres, J. L.; Head-Gordon, M.; Replogle, E. S.; Pople, J. A. *Gaussian 98*, revision A.7; Gaussian, Inc.: Pittsburgh, PA, 1998.

(17) Andersson, K.; Blomberg, M. R. A.; Fulscher, M. P.; Karlstrom, G.; Lindh, R.; Malmqvist, P.-A.; Neogrady, P.; Olsen, J.; Roos, B. O.; Sadlej, A. J.; Schutz, M.; Seijo, L.; Serrano-Andres, L.; Siegbahn, P. E. M.; Widmark, P.-O. *MOLCAS*, version 4; Lund University: Lund, Sweden, 1997.

(18) (a) Matsuzawa, H.; Iwata, S. *Chem. Phys.* **1992**, *163*, 297. (b) Ruiz, E.; Salahub, D. R.; Vela, A. *J. Am. Chem. Soc.* **1995**, *117*, 1141. (c) Ruiz, E.; Salahub, D. R.; Vela, A. *J. Phys. Chem.* **1996**, *100*, 12265. (d) Kang, H. C. *Chem. Phys. Lett.* **1996**, *254*, 135.

(19) (a) Bloemink, H. I.; Hinds, K.; Legon, A. C.; Thorn, J. C. *Chem. Phys. Lett.* **1994**, *223*, 162. (b) Bowmaker, G. A.; Boyd, P. D. W. *J. Chem. Soc., Faraday Trans.* **1987**, *83*, 2211.

(20) Xu, S. C. *J. Chem. Phys.* **1999**, *111*, 2242.